Electric Power Systems Research 199 (2021) 107393

Contents lists available at ScienceDirect

Electric Power Systems Research

journal homepage: www.elsevier.com/locate/epsr

Assessing the benefits of exchanging spinning reserve capacity within the hydro-Dominated nordic market

Arild Helseth [*,a], Mari Haugen [a], Hossein Farahmand [b], Birger Mo [a], Stefan Jaehnert [a], Inge Stenkløv [c]

[a] SINTEF Energy Research, Trondheim 7465, Norway
[b] Department of Electric Power Engineering, Norwegian University of Science and Technology, Trondheim 7495, Norway
[c] Statnett, 0423 Oslo

ARTICLE INFO

Keywords:
Hydroelectric power generation
Power generation economics
Unit commitment and dispatch
Reserve capacity

ABSTRACT

This paper presents a hydrothermal scheduling toolchain suitable for detailed studies of procurement of spinning reserves in the hydro-dominated Nordic power system. The toolchain combines a long-term model to find the expected marginal value of water in the hydropower reservoirs and initial states for thermal generators, and a short-term model to optimize the daily unit commitment and dispatch. The short-term model has a detailed description of both hydro and thermal generation technologies to realistically constrain their capabilities as reserve capacity providers. The toolchain is applied on a data description representing a 2030 scenario of the Northern European power system to quantify the benefits of exchanging spinning reserve capacity both between bidding zones and between countries within the Nordic market. By allowing 10% of the transmission line capacity for exchange of reserves, we find that the daily average economic benefit is 290 k€ and 102 k€ for reserve exchange between bidding zones and countries, respectively. Moreover, we quantify and illustrate the importance of applying unit commitment for hydropower stations and strictly enforcing their minimum power requirements.

1. Introduction

In the transition towards a low-carbon European power system, increasing shares of wind power in the system, retirement of thermal and nuclear power plants and increasing exchange capacities due to new interconnectors, are all examples of the structural system changes that are going to take place. Along with these structural changes, there is an increasing need for fast-responding reserves in the power system to ensure system security.

Increasing exchange capacity between countries amplifies the possibility to trade reserve capacity and balancing energy across borders. Cross-border balancing allows more efficient use of the system resources, which in turn has the potential to lower the overall need for reserve capacity and increase the level of reliability [1]. Traditionally, the procurement of reserves in Europe has been seen as a national task, leading to suboptimal solutions, as quantified in [2]. This practice is currently under change, guided by the European Union's *Electricity Balancing Network Code* (EBGL) [3], aiming at integration of balancing markets to enhance the efficiency of the European balancing processes.

In the Nordic system, the transmission system operators (TSOs) are responsible for matching supply and demand of electricity in real time. To ensure this balance, the TSOs need to be able to acquire balancing services, both in terms of reserve capacity and balancing energy. The market framework and market clearing sequences adopted in the Nordic system are described in [4–6]. Currently, reserve capacity is procured on a national level, and volume requirements for specific bidding zones within each country are being developed. As an example, the Norwegian TSO (Statnett) procures primary (FCR) and secondary reserves (aFRR) for Norway through market-based approaches using the marginal pricing principle [7]. The availability of flexible providers of spinning reserve capacity varies significantly across the Nordic market zones, from the hydro-dominated areas in Western Norway and Northern Sweden, to the load centers in South-East. Following up on the EBGL, the Nordic TSOs proposed a methodology for allocation of cross-zonal capacity for exchange of balancing capacity to ease the provision of aFRR [8].

* Corresponding author.
E-mail address: arild.helseth@sintef.no (A. Helseth).

https://doi.org/10.1016/j.epsr.2021.107393
Received 20 November 2020; Received in revised form 16 April 2021; Accepted 26 May 2021
Available online 9 June 2021

In this study we consider spinning reserve capacity (typically FCR and aFRR) as a generic product, and assess the potential for reducing system variable costs when allowing the exchange of such reserve capacity over existing power lines between bidding zones and countries in the Nordic power market. We emphasize the point that this potential cannot be accurately assessed without detailed treatment of the hydropower system with its many complex cascade arrangements. For this purpose we apply a hydrothermal scheduling toolchain comprising a long-term model to find the expected marginal value of stored water in the reservoirs and initial states for thermal generators, and a short-term model to optimize the daily operation for selected representative days.

A mapping of recent power system models is presented in [9], and a brief discussion on the ones that we find most relevant in this context is provided below. In particular, the toolchain presented in this paper has similarities to the toolchain developed within the research project 'Wind power integration in a liberalised electricity market' (WILMAR), detailed in [10,11]. The WILMAR toolchain combines a short-term multi-market model [10] with a long-term model [11] to address the importance of both short-term uncertainties (in wind power and demand) and long-term dynamics in hydro storages. To account for the value of having power plants online as well as energy stored in heat and electricity storages at the end of the planning horizon, the WILMAR toolchain uses dual values obtained for these storages in the previous planning loop. The short-term model is further refined to include unit commitment decisions on thermal generators in [12]. The METIS short-term power market model uses weather scenarios to simulate the market clearing and reserve procurement in the European system [13,14], but has a simplified representation of long-term hydropower storages based on guide curves. Similar approximations of hydropower representations are made in the detailed market simulation models Antares [15] and SiSTEM [16].

In [17] the potentials for reduction of balancing costs through a common Northern European balancing (or secondary control) market is investigated, assessing the relationship between balancing cost and the available share of transmission capacity for exchange of balancing energy. A toolchain combining a long-term hydrothermal scheduling tool and a separate model for reserve procurement and system balancing was presented in [18]. Our work differs from [18] in the more detailed treatment of hydropower and in allowing reserve capacity procurement impacting the energy prices through a co-optimization of these two "products". The implications of cross-border transmission capacity reservation for aFRR exchange within the Northern European power system is presented in [19]. The authors aim at recreating today's sequential market design for reserve procurement and the day-ahead energy market clearing. A three-step approach was taken, where first the future spot market energy prices are estimated, then reserves are procured, and finally the dispatch. In [1] the value of inter-zonal coordination of reserve sizing, procurement and activation is investigated in the European market context. In [20] the timing of procuring reserves is analyzed, comparing the impact of procuring reserves before, together with and after the energy-market clearing. Recently, [21] studied the impacts of an integrated European intraday market, emphasizing the flexibility provided by pumped storage hydropower. A detailed market simulator involving short-term scheduling of hydropower system in day-ahead and real-time markets was presented in [22], relying on water values computed in a separate and less detailed procedure for the aggregated hydropower system.

In our work, we go a step further in representing the detailed hydropower throughout the toolchain to realistically represent the available flexibility associated with hydropower operation.

The contributions of this work are twofold:

- We present a toolchain combining long- and short-term hydrothermal scheduling models in a consistent manner to quantify the benefit of exchanging spinning reserve capacity across bidding zones and countries in the Nordic power market. The toolchain framework has been presented in our previous works [23,24], but the coupling between the long- and short-term models are further elaborated here. Moreover, the short-term model is extended by modelling the unit commitment decisions for hydropower stations as well as detailed constraints for the exchange of reserve capacity between countries and bidding zones.
- We assess the benefits of exchanging spinning reserve capacity between bidding zones and countries within the Nordic market for a set of representative days for a scenario of the 2030 Northern European power system. To the best of our knowledge, this type of assessment has not been reported in the technical literature using models and toolchains with similar level of detail on both the hydro and thermal generation system.

2. Mathematical model

We apply a fundamental hydrothermal scheduling toolchain, combining a long-term model briefly described in Section 2.1 and a short-term model detailed in Sections 2.2 and 2.3.

2.1. Long-Term model

The long-term hydropower scheduling problem is complex due to the coupling in time between hydropower reservoirs, and the high degree of uncertainty in the future weather conditions. The operational decision in one time period will affect the reservoir levels in the next period, and this coupling in time between hydropower reservoir levels makes the problem dynamic. The problem is also stochastic because future uncertainty must be considered when decisions are made. Typically, future values of weather-related input data (such as inflow, snow, wind, solar radiation and temperature) as well as exogenous power prices are considered uncertain, and will affect the strategy for operating the hydropower reservoirs. Therefore, the problem is normally solved by some variant of the stochastic dynamic programming algorithm [25].

The long-term model used in this framework is the Scenario Fan Simulator (FanSi) model described in [23]. The FanSi model solves a two-stage stochastic linear programming (LP) problem to determine the decisions for each week. Uncertainties in weather and exogenous power prices are considered and represented by a fan of scenarios. From the long-term model a set of Benders cuts of type (1) is found for each week t. These cuts describe the future expected cost function (FCF) α_{t+1} of operating the system the remaining period of analyses seen from the beginning of the next week $t+1$. The FCF is expressed as a function of what we will here refer to as the *long-term state variables*; The hydro storage levels v_{ht} for all reservoirs $h \in \mathscr{H}$ at the end of the week t. The cuts in (1) are created and used for specific scenarios of stochastic variables, and therefore there is no need to treat these stochastic variables as state variables. The cut coefficients π_{hc} (water values) and the intercept β_c are cut parameters computed by the FanSi model.

$$\alpha_{t+1} + \sum_{h \in \mathscr{H}} \pi_{hc} v_{ht} \geq \beta_c \quad \forall c \tag{1}$$

2.2. Short-Term model

A short-term model with more technical details and finer time resolution is used to compute the daily unit commitment and dispatch for the same system and system boundary considered by the long-term model. A first version of the model was presented in [26] and later updated in [24]. It is further improved in this work, detailing the unit commitment of hydropower stations and the nonconvex hydropower production function as described in Section 2.3 and the possibility to exchange reserve capacity between countries and bidding zones. The short-term model is coupled with the long-term strategic model through the Benders cuts in (1) referring to the end of the week, as illustrated in Fig. 1.

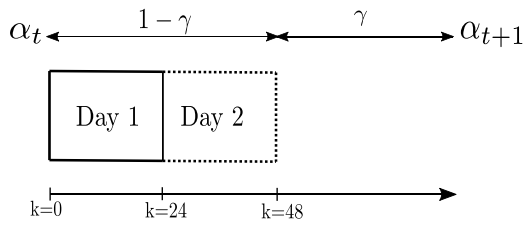

Fig. 1. Illustration of coupling between short- and long-term models.

The short-term problem is formulated as a deterministic MIP problem considering a 48 h time horizon. The decisions from the first 24 hours are stored, as illustrated in Fig. 1. The last 24 hours in each problem serve the purpose of valuating the *short-term state variables* that are not considered as state variables in the FCF. In this work these are the thermal and hydropower unit commitment status variables, as well as power and water flows that are subject to ramping constraints.

A linear interpolation in the FCFs of type (1) between two consecutive weeks was used to account for seasonal variations in water values, as indicated in Fig. 1 and represented in (2) in Section 2.3. This concept was first introduced in [24]. As an example, the fraction γ equals $\frac{5}{7}$ for Monday, $\frac{4}{7}$ for Tuesday, and so on.

Long-term state variables (reservoir volumes) are passed from the long-term to the short-term model, while the short-term state variables (hydro and thermal commitment statuses, and power and water flows subject to ramping constraints) are obtained in an iterative approach as follows: First we solve the short-term problem by letting the short-term state variables take the values indicated by the long-term model. Since states from the long-term model are continuous we decided to turn on partially started units and stations. Subsequently, we solve the short-term problem and use the short-term state variables at the end of the first day as initial states when solving the short-term problem a second time. This last step is particularly important for thermal units with high start/stop costs, where the partial startups suggested from the long-term model should be refined.

The short-term model uses the same data sources as used in the long-term model, with the addition of some extra details describing the generation technologies. The short-term model is implemented in the high-level open-source modeling language Pyomo [27] and uses CPLEX [28] as the optimization solver.

2.3. Short-Term problem formulation

This section presents the mathematical formulation of the two-day optimization problem that is solved for each representative sequence in the short-term model. The formulation represents a deterministic unit commitment model jointly optimizing the use of energy and procurement of spinning reserve capacity. The problem is defined for a set of $\mathscr{A}$ bidding zones using $\mathscr{K}$ time steps. We let $\mathscr{H}$ and $\mathscr{G}$ be the sets of hydropower stations and thermal generating units, respectively, while $\mathscr{D}$ denotes the set of price-elastic demands. We use hourly time resolution for both days, so $|\mathscr{K}| = 48$. Units are in MW (power), MWh (energy), Mm^3 (water volume and inflows), m^3/s (water flows) and 10^3 € (costs). Γ_k denotes the conversion between water flow in m^3/s and water volume in Mm^3. All variables (except the FCF α) in the model are non-negative, and many have time-dependent lower and upper boundaries which are not explicitly stated here. To ease the formulation, but without loss of generality, we omit the conversion between power and energy by assuming a time-step length of one hour.

2.3.1. Objective

The objective in (2) is to minimize the system costs associated with unit commitment and dispatch of the system over a two-day period and the expected cost of operating the system in the future. The cost elements represented in the objective function are the start-up cost (c^S) of thermal and hydropower units, generation p_{gk} from thermal units at a marginal cost C_g^G, curtailment y_{ak}^E of price-inelastic demand at cost C_a^E, relaxation of the up (y_{ak}^{R+}) and down (y_{ak}^{R-}) reserve requirements at cost C_a^R, and meeting the price-elastic demand y_{dk}^D with value C_{dk}^D. The future expected operating cost is interpolated between α_t and α_{t+1} with the fraction γ in (2), and these are constrained by Benders cuts in (1).

$$Z_t = \min \sum_{k\in\mathscr{K}} \Bigg(\sum_{j\in\mathscr{H}\cup\mathscr{G}} c_{jk}^S + \sum_{g\in\mathscr{G}} C_g^G p_{gk} + \sum_{a\in\mathscr{A}} \Big(C_a^E y_{ak}^E + C_a^R y_{ak}^{R+} + C_a^R y_{ak}^{R-} \Big) - \sum_{d\in\mathscr{D}} C_{dk}^D y_{dk}^D \Bigg) + \gamma\alpha_t + \Big(1-\gamma\Big)\alpha_{t+1} \tag{2}$$

2.3.2. Hydropower constraints

The hydropower system is modeled using the building blocks of hydropower *modules* h connected through the three waterways discharge (q^D), bypass (q^B) and spillage (q^S), as represented by equations (3). A module comprises one reservoir and one power station, and has a set of upstream modules Ω_h from which it receives water through one or more of the waterways. Constraint (3a) balances the reservoir volume (v_{hk}) with spillage and release decisions (q^R) and regulated inflow (I_{hk}^R), while (3b) balances the reservoir release with unregulated inflow (I_{hk}^U), discharge and bypass. The discharge (3c) and bypass (3d) variables are often subject to seasonal variations in both lower ($\underline{Q}^D, \underline{Q}^B$) and upper ($\overline{Q}^D, \overline{Q}^B$) boundaries to ensure that watercourses are operated in a sustainable manner. Some rivers have releases in consecutive periods constrained by a maximum allowed ramping rate ($\Delta_{Q_h^R}$) as in (3e).

$$v_{hk} - v_{h,k-1} + \Gamma_k\big(q_{hk}^R + q_{hk}^S\big) - \Gamma_k\Bigg(\sum_{j\in\Omega_h^D} q_{jk}^D + \sum_{j\in\Omega_h^B} q_{jk}^B + \sum_{j\in\Omega_h^S} q_{jk}^S\Bigg) = I_{hk}^R \;\; \forall h,k \tag{3a}$$

$$\Gamma_k\big(q_{hk}^B + q_{hk}^D - q_{hk}^R\big) = I_{hk}^U \qquad \forall h,k \tag{3b}$$

$$\underline{Q}_h^D \le q_{hk}^D \le \overline{Q}_h^D \qquad \forall h,k \tag{3c}$$

$$\underline{Q}_h^B \le q_{hk}^B \le \overline{Q}_h^B \qquad \forall h,k \tag{3d}$$

$$-\Delta_{Q_h^R} \le q_{hk}^R - q_{h,k-1}^R \le \Delta_{Q_h^R} \qquad \forall h,k \tag{3e}$$

$$q_{hk}^D = u_{hk}\underline{Q}_h^{D*} + \sum_{n\in\mathscr{N}_h} q_{nhk}^D \qquad \forall h,k \tag{3f}$$

$$0 \le q_{nhk}^D \le \overline{Q}_{nhk}^D u_{hk} \qquad \forall n,h,k \tag{3g}$$

$$p_{hk} = u_{hk}\underline{P}_h + \sum_{n\in\mathscr{N}_h} \eta_{nh} q_{nhk}^D \qquad \forall h,k \tag{3h}$$

$$p_{hk} + r_{hk}^+ \le \overline{P}_h u_{hk} \qquad \forall h,k \tag{3i}$$

$$\underline{P}_h u_{hk} \le p_{hk} - r_{hk}^- \qquad \forall h,k \tag{3j}$$

$$c_{hk}^S \ge C_h^S\big(u_{hk} - u_{h,k-1}\big) \qquad \forall h,k \tag{3k}$$

Eqn. (3f) -(3k) constrain the operation of the hydropower station, and are elaborated in the next paragraphs. In practice a hydropower station comprises many units (or aggregates), and for fine precisions in the calculations, the individual units should be represented, as detailed in [29]. For the large-scale system considered here with more than 1000 modules, a unit-based approach was not possible. This is primarily due to lack of detailed data, but also due to the significant increase in

computational complexity. An approximate curve representing the power output as a function of station discharge (PQ curve) is presented instead, as explained in the following. A station with several units will have a best efficiency point for each combination of units. This is illustrated in Fig. 2 where the output from two units loaded in sequence is shown as the grey-dotted line with best efficiency points B and C. A linear approximation of the PQ-curve in Fig. 2 uses the points B, C and D, which is a good approximation when the units are operated at their best efficiency points B and C. However, if the station has to run on low output, e.g., close to point A, to deliver down-regulation reserves or to meet a minimum discharge requirement, the power output is over-estimated with the linear approach. To reflect this, we introduce a minimum discharge ($\underline{Q}_h^{D*}$)[1] and power output ($\underline{P}_h$) and model the station's power output as in (3f)-(3h). This corresponds to the curve defined by the points A, B, C and D.

The PQ-curve is scaled according to the actual head at the beginning of the day. This is a simplification, assuming that the relative head will vary little during the day, which is typically the case for the many high-head stations in Norway.

The unit commitment of the hydropower station is controlled by the binary variable u_{hk}, indicating if the station is running. The power output from a station h above its minimum generation level is described as a piecewise linear and concave functional relationship of station discharge. The discharge variable is segmented in $\mathscr{N}_h$ segments as shown in (3f), where the use of each segment n is limited by a maximum limit ($\overline{Q}_n^D$) in (3g). The power output is described in (3h), where η_{nh} represents the efficiency (MW/m^3/s) per discharge segment n. Spinning reserves can be provided by stations, both upwards (r_{hk}^+) in (3i) and downwards (r_{hk}^-) in (3j). When allowing separate reservation of up- and down-regulation per station, there may be some stations that are more frequently committed in one particular direction, possibly leading to a nonzero energy impact. Such effects are not captured in this model, since the activation of reserves is not considered. Start-up cost of a station is represented by variable c_{hk}^S in (3k) according to a cost C_h^S per start-up. Pumps and pumped-storage power plants are not included in the formulation above for brevity.

2.3.3. Thermal constraints

Thermal units are modeled in (4) according to the equations in [30] (Chapter 5.3.1–5.3.4) and as further discussed in [24]. Maximum ramping rates up (S_g^U) and down (S_g^D) as well as maximum start-up (P_g^{SU}) and shut-down (P_g^{SD}) ramping capacities are provided per thermal unit. Minimum up- and down-times are imposed to reduce component stress.

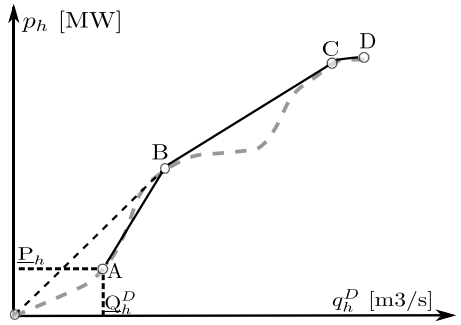

Fig. 2. Illustration of the relationship between discharge and power output for a hydropower station.

[1] Note that $\underline{Q}_h^{D*}$ is a technical limit while $\underline{Q}_h^D$ in (3c) is an environmental limit, and that they generally differ.

We introduce a set of parameters indicating the minimum number of hours a unit needs to be up if started (T_g^U) or down if shut-down (T_g^D), and the minimum number of hours that a unit needs to be up from the beginning of the optimization horizon if it is initially up (T_g^{U0}) or down (T_g^{D0}) if its initially down. Moreover, we let $T = |\mathscr{K}|$ and define the following parameters: $T_g^{Ue} = \min(T, T_g^{U0})$ and $T_g^{De} = \min(T, T_g^{D0})$.

$$u_{g,k-1} - u_{gk} + z_{gk}^U - z_{gk}^D = 0 \qquad \forall g,k \tag{4a}$$

$$z_{gk}^U + z_{gk}^D \le 1 \qquad \forall g,k \tag{4b}$$

$$p_{gk} + r_{gk}^+ \le \overline{P}_g u_{gk} \qquad \forall g,k \tag{4c}$$

$$\underline{P}_g u_{gk} \le p_{gk} - r_{gk}^- \qquad \forall g,k \tag{4d}$$

$$p_{gk} - p_{g,k-1} \le S_g^U u_{g,k-1} + P_g^{SU} z_{gk}^U \qquad \forall g,k \tag{4e}$$

$$p_{g,k-1} - p_{gk} \le S_g^D u_{gk} + P_g^{SD} z_{gk}^D \qquad \forall g,k \tag{4f}$$

$$\sum_{k=1}^{T_g^{Ue}} u_{gk} = T_g^{Ue} \qquad \forall g \tag{4g}$$

$$\sum_{k'=k}^{k+T_g^U-1} u_{gk'} \ge T_g^U z_{gk}^U \qquad \forall g, k = T_g^{Ue}+1,\ldots,T-T_g^U+1 \tag{4h}$$

$$\sum_{k'=k}^{T} \left(u_{gk'} - z_{gk}^U\right) \ge 0 \qquad \forall g, k = T-T_g^U+2\ldots,T \tag{4i}$$

$$\sum_{k=1}^{T_g^{De}} u_{gk} = 0 \qquad \forall g \tag{4j}$$

$$\sum_{k'=k}^{k+T_g^D-1} \left[1 - u_{gk'}\right] \ge T_g^D z_{gk}^D \qquad \forall g, k = T_g^{De}+1,\ldots,T-T_g^D+1 \tag{4k}$$

$$\sum_{k'=k}^{T} \left(1 - u_{gk'} - z_{gk}^D\right) \ge 0 \qquad \forall g, k = T-T_g^D+2,\ldots,T \tag{4l}$$

We introduce three binary variables indicating if the unit is on (u_{gk}), started up (z_{gk}^U) or shut-down (z_{gk}^D) at the beginning of time step k, controlled by (4a) and (4b). Spinning reserves can be provided both upwards (r_{gk}^+) in (4c) and downwards (r_{gk}^-) in (4d). The constraints (4e) and (4f) limit upward and downward ramping, respectively. The minimum up- and down-times for thermal units are enforced by (4g)-(4i) and (4j)-(4l), respectively.

2.3.4. System-Wide constraints

Power balances for each bidding zone in each time step are provided in (5). Thermal and hydro generations are scheduled to meet the net load, i.e., the demand (D_{ak}) subtracted the wind power (P_{ak}), while allowing power exchange (f) with neighboring bidding zones. The ability to curtail (y_{ak}^E) energy at a high cost and dump (d_{ak}) power at a zero cost provides the price roof and floor, respectively.

$$\sum_{g\in\mathscr{G}_a} p_{gk} + \sum_{h\in\mathscr{H}_a} p_{hk} - \sum_{d\in\mathscr{D}_a} y_{dk}^D + \sum_{\substack{\ell:(a,b)\\ \in\mathscr{L}_a}} \left[(1-\zeta_\ell) f_{bak} - f_{abk}\right] + y_{ak}^E - d_{ak} = D_{ak} - P_{ak} \qquad \forall a,k \tag{5}$$

The transmission system is described by a set of connections $\ell \in \mathscr{L}$, and the subset of connections $\mathscr{L}_a$ is associated with each bidding zone a. We let $\mathscr{L} = \mathscr{L}^{AC} \cup \mathscr{L}^{DC}$ comprise both AC ($\mathscr{L}^{AC}$) and HVDC ($\mathscr{L}^{DC}$) connections. Each connection $\ell : (a,b)$ has two directional flow variables: f_{ab} and f_{ba}. Exchange of up- (f^{+}_{abk}) and down-regulating (f^{-}_{abk}) reserve capacity can be allocated each AC connection, according to (6a), (6b) and (6e), bounded by the transmission capacity (F). Exchange of reserves are not allowed on HVDC connections in (6c). The transmission losses depend linearly on the flows by a loss fraction (ζ_ℓ) in (5). Ramping limits on HVDC connections between external markets and bidding zones are constrained by a maximum ramping rate (Δ_ℓ) in (6d). The exchange of reserve capacity is limited to a fraction ϕ of the total transmission capacity in (6e).

$$0 \le f_{abk} + f^{+}_{abk} \le F_{abk} \quad \forall \ell : (a,b) \in \mathscr{L}^{AC} \tag{6a}$$

$$0 \le f_{bak} + f^{-}_{abk} \le F_{bak} \quad \forall \ell : (a,b) \in \mathscr{L}^{AC} \tag{6b}$$

$$0 \le f_{abk} \le F_{abk} \quad \forall \ell : (a,b) \in \mathscr{L}^{DC} \tag{6c}$$

$$-\Delta_\ell \le \left(f_{abk} - f_{bak}\right) - \left(f_{ab,k-1} - f_{ba,k-1}\right) \le \Delta_\ell \quad \forall \ell : (a,b) \in \mathscr{L}^{DC} \tag{6d}$$

$$0 \le f^{+}_{abk}, f^{-}_{abk} \le \phi F_{abk} \quad \forall \ell : (a,b) \in \mathscr{L}^{AC} \tag{6e}$$

We consider spinning reserve capacity as a generic product, resembling the joint requirement for FCR and aFRR reserve capacity. Reserve requirements for spinning upward (R^{+}_{c}) and downward (R^{-}_{c}) reserves are defined per group c of bidding zones in (7) and (8). In the case study in Section 3 we either treat all bidding zones within each country as a group or each bidding zone as a group. A pre-defined set of hydropower plants ($h \in \mathscr{H}^{R}_{a}$) and thermal power plants ($g \in \mathscr{G}^{R}_{a}$) are allowed to deliver spinning reserve capacity. We allow for relaxation of the requirements in (7) and (8) through variables y^{R+}_{ak} and y^{R-}_{ak}, respectively. By letting the cost C^{R}_{a} of using y^{R+}_{ak} and y^{R-}_{ak} be marginally lower than the energy rationing cost C^{E}_{a} in (2), we ensure that (7) and (8) are relaxed before rationing price-inelastic demand.

$$\sum_{a \in \mathscr{A}^{R}_{c}} \left(\sum_{h \in \mathscr{H}^{R}_{a}} r^{+}_{hk} + \sum_{g \in \mathscr{G}^{R}_{a}} r^{+}_{gk} + y^{R+}_{ak} \right) + \sum_{a \in \mathscr{A}^{R}_{c}} \sum_{\substack{\ell:(a,b) \\ \in \mathscr{L}^{R}_{a}}} \left(f^{+}_{bak} - f^{+}_{abk} \right) \ge R^{+}_{c} \quad \forall c,k \tag{7}$$

$$\sum_{a \in \mathscr{A}^{R}_{c}} \left(\sum_{h \in \mathscr{H}^{R}_{a}} r^{-}_{hk} + \sum_{g \in \mathscr{G}^{R}_{a}} r^{-}_{gk} + y^{R-}_{ak} \right) + \sum_{a \in \mathscr{A}^{R}_{c}} \sum_{\substack{\ell:(a,b) \\ \in \mathscr{L}^{R}_{a}}} \left(f^{-}_{bak} - f^{-}_{abk} \right) \ge R^{-}_{c} \quad \forall c,k \tag{8}$$

Where the set A^{R}_{c} comprises all zones in a group c and the set $\mathscr{L}^{R}_{a}$ comprises all lines connecting from zone a in reserve group c to another reserve group.

2.4. Solution approach

The applied toolchain comprises a long-term model briefly described in Section 2.1 and a short-term model elaborated in Section 2.3. The long-term model is run first to find strategies in the form of Benders cuts in (1). Subsequently, the short-term model re-optimizes representative short-term sequences using the Benders cuts as input. While the long-term model is stochastic and based on linear programming, the short-term is deterministic, has a finer time resolution, is more constrained, and is formulated as a MIP problem. In particular, the long-term model does not cover the following constraints and variables described in Section 2.3:

- *Hydropower:* (3e), variables u_{hk}, r^{+}_{hk} and r^{-}_{hk}. The production function in (3f)-(3h) becomes slightly different, see [23] for details.
- *Thermal:* (4a)-(4b) and (4e)-(4l), variables u_{gk}, z^{U}_{gk}, z^{D}_{gk}, r^{+}_{gk} and r^{-}_{gk}.
- *System wide:* (6d)-(6e),(7) and (8), variables f^{+}_{abk}, f^{-}_{abk}, y^{R+}_{ak} and y^{R-}_{ak}.

In this work we experiment with three different solution strategies for solving the short-term optimization problem described in Section 2.3:

1. As an MIP problem, denoted MIP.
2. As an MIP problem relaxing the integrality requirement for the binary variables associated with hydropower operation, so that $u_{hk} \in [0,1]$, denoted HLP.
3. As an LP problem, relaxing the integrality requirement for the binary variables associated with both hydropower stations and thermal units, denoted LP.

Using the MIP strategy will provide the most accurate result, but may in some cases be computationally prohibitive. The HLP and LP strategies are computationally much faster. In Section 3 we compare the results of the two latter with the MIP strategy to evaluate their appropriateness for this type of study.

3. Case study

3.1. Data description

A data description of a future scenario of a low-emission Northern European power system for year 2030 was used in this case study. A brief presentation of this scenario is provided in the following, the reader is referred to [31] for more details. The system boundary is illustrated in Fig. 3, where the darker color reflects the countries represented by a higher level of detail. The current 11 bidding zones within the Nordic

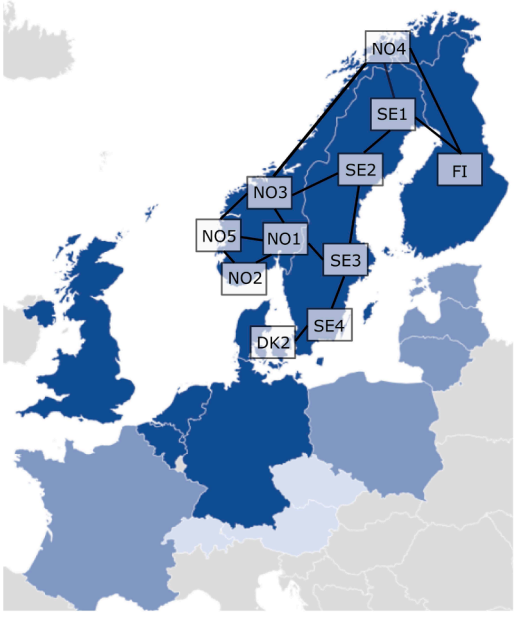

Fig. 3. Case study system boundary. The Nordic bidding zones and their interconnections are indicated.

synchronous system are shown in the figure.

The data description comprises a detailed representation of the Nordic hydropower system, with 1093 hydropower modules, most of which are part of complex cascades. To limit the number of binary variables, only the 292 modules with more than 20 MW installed capacity and 2 Mm^3 storage capacity were represented with binary commitment variables. These modules were allowed to deliver spinning reserve capacity. We assumed their minimum generation to be at 50% of the best efficiency point, and a 20% reduction in efficiency when operating at minimum generation (point 'A' in Fig. 2) compared to the best efficiency.

A total of 252 thermal units were represented with start-up costs, minimum up- and down-times, and ramping constraints. A set of 26 flexible thermal units were allowed to deliver spinning reserve capacity within the Nordic system in the case study.

The total amount of installed wind and solar generation capacity is based on recent European political targets and commitments, and amounts for 30 % of the expected electricity generation. Renewable power generation accounts for 54 % of the expected electricity generation. More details on the data description can be found in [31].

The combined weather uncertainty in space and time was accounted for using 58 historical weather years. The weather years represent uncertainty and natural variation in inflow to the individual hydropower reservoirs, wind and solar power generation, and temperature that affect the load. Hourly wind and solar generation are calculated based on Reanalysis data (https://reanalyses.org/) with a spatial resolution of 2.5 degrees both in latitude and longitude [32].

This data description also includes assumptions for demand, transmission capacity between the bidding zones, fuel prices and the CO_2 price for the year 2030 [31]. Nuclear power is assumed decommissioned in Germany, but remains an important generation technology in several countries, such as Great Britain. With a substantial amount of other thermal power generation remaining in the system, fuel and CO_2 prices still have an important impact on the power prices. A CO_2 price of 30 € /ton, a gas fuel price of 20 € /MWh and a coal price of 70 € /ton were assumed.

The modeled spinning reserve requirements for the current bidding zones within the Nordic synchronous system are shown in Table 1. We underline that both the bidding zone configuration and the requirements are uncertain towards 2030. We assume that the requirements are static in time and symmetric for up- and down-regulating reserves. The requirements are based on today's requirements for FCR and aFRR reserves and known plans for changing those. We expect that the demand for aFRR will double from 300 MW to 600 MW for the Nordic regions by 2030 [33]. Estimated factors for distribution of this demand per bidding zone and country were provided by Statnett. The demand for FCR was assumed to be as today; 600 MW in total for FCR-N (normal primary reserves, symmetric) and 1200 MW for FCR-D (contingency primary reserves, upward). The distribution of demand for primary reserves between countries was taken from [6]. Because of new interconnectors built to exogenous markets by 2030, we chose to add a requirement for 1200 MW FCR-D down. This product in not implemented today but will probably be implemented after North Sea Link and NordLink come into operation. The models used in this study do not differentiate between primary and secondary reserves, so the individual reserve requirements (for aFRR, FCR-N and FCR-D) were merged into one common reserve requirement per bidding zone and country, leading to the numbers in Table 1.

Table 1
Spinning reserve requirements.

Country	Bidding zone	Requirement [MW]
Norway	NO1	167
	NO2	229
	NO3	83
	NO4	146
	NO5	167
Sum		**792**
Sweden	SE1	216
	SE2	157
	SE3	354
	SE4	197
Sum		**924**
Finland	FI	**335**
Denmark	DK2	**356**
Sum		**2407**

3.2. Selection of test cases

We selected 3 different inflow years, representing years with low (1969), medium (2013) and high (2011) total inflow volumes to the Nordic hydropower reservoirs. A set of 4 representative weeks, representing winter (week 9), spring (week 20), summer (week 31) and autumn (week 45), were selected to account for seasonal patterns in model input, such as demand, inflow and solar power. The FanSi long-term model was run to provide cuts as showed in Eq. (1) representing the expected value of water for the representative years and weeks. For each of these weeks, Monday (D1) and Saturday (D6) were considered as representative week and weekend days, respectively. In total, this summed up to 24 ($3 \times 4 \times 2$) representative days to be considered. Recall that each representative day is treated as the first day in a two-day sequence being optimized in the short-term model.

For each of the 24 representative days we considered reserve requirements both per bidding zone and per country, according to Table 1. Moreover, for each case we tested 4 different values (0.0, 0.05, 0.10 and 0.15) of the transmission capacity fraction (ϕ) made available for exchange of reserves through AC connections. Finally, to check the importance of using binary variables in the modelling of thermal units and hydropower stations we ran separate cases using the MIP, HLP and LP strategies described in Section 2.4.

All results presented in the following are obtained by the MIP strategy unless explicitly stated otherwise. Energy and reserve capacity are co-optimized according to the problem formulation in Section 2.3, using cuts obtained from the FanSi long-term model introduced in Section 2.1.

3.3. Results

Table 2 shows the reduction in unit commitment and dispatch costs for each representative day when allowing 10% of the transmission line capacity for exchange of reserves and when using the MIP strategy, compared to the base case where no reserves are exchanged. The highest benefit is obtained in the summer (week 31) period, while the lowest benefit was seen for the winter period (week 9). As expected, the benefit of allowing reserve exchange is higher when considering reserve requirements per bidding zone rather than per country, since the latter case allows bidding zones within each country to share reserves. Assuming 5 weekdays like D1 and 2 weekend days like D6 in a representative week and giving equal weight to each representative week, the average daily cost savings are 290 k€ and 102 k€ when considering

Table 2
Economic benefit of reserve exchange (in k€).

		Bidding Zone			Country		
Day	Week	Dry	Med	Wet	Dry	Med	Wet
D1	9	106	126	83	29	46	38
D1	20	318	390	229	88	164	96
D1	31	341	712	288	145	143	104
D1	45	149	121	84	45	71	36
D6	9	113	220	168	58	57	103
D6	20	645	315	421	195	179	102
D6	31	546	701	696	127	215	150
D6	45	615	268	184	214	121	90

exchange of reserves per bidding zone and country, respectively.

On average, the HLP and LP relaxations provided a cost reduction at 10% reserve exchange that was 78% and 71% of the cost reduction from the MIP solution in Table 2, respectively.

Fig. 4 shows the cost reductions for a summer weekday in the wet scenario with different fractions of transmission capacity allowed for reserve exchange between bidding zones using different strategies (MIP, HLP and LP). A substantial decrease in cost reduction is observed when gradually increasing the fraction of transmission capacity available for reserve exchange. This pattern was found in many of the other cases as well, and generally indicates that a major part of the potential economic gain of reserve exchange can be harvested by allowing approximately 10% of the transmission capacity for exchange of reserves. Fig. 4 shows significantly lower cost reductions obtained from using the LP and HLP strategies compared to the MIP strategy. A similar pattern was found in most cases, but we also identified days for which the cost reductions were lower when using the MIP strategy than with HLP and LP. As a reference, with no reserve requirement at all (i.e. $R_c^+ = R_c^- = 0$ in (7)-(8)), the cost reduction was 492 k€ /day. This value reflects the cost of having a reserve requirement per bidding zone without the possibility to exchange reserves for this particular day.

Relaxation of the reserve requirements in (7) and (8) was not observed, i.e., the variables y_{ak}^{R+} and y_{ak}^{R-} were zero in all cases. By letting C_a^R take a value marginally below the rationing cost, we have chosen a rather strict enforcement of the reserve requirements. In Fig. 5 the benefit of 10% reserve exchange for D1 in week 31 for the normal inflow year is found for different values of C_a^R. When C_a^R takes values lower than 900 € /MWh, the reserve constraints are gradually relaxed, until fully relaxed when C_a^R=0. For values varying between 900 and 0 € /MWh, C_a^R becomes lower than the marginal cost of electricity for certain hours, activating the use of variables y_{ak}^{R+} and y_{ak}^{R-}, and decreasing the economic benefit of reserve exchange.

Fig. 6 shows the procurement of reserves per technology for a specific hour in the dry scenario in week 31 when allowing 10% of the transmission capacity for exchange of reserves. The net exchanges of reserves per bidding zone are indicated in the top (up-regulation) and bottom (down-regulation) of the figure, where a positive value means that the bidding zone imports reserve capacity, and vice versa. The hydropower-dominated bidding zones NO2, NO3, NO5, SE1 and SE2 are the exporters of up-regulating reserve capacity, while NO1, NO4, SE3, SE4, DK2 and FI are importers. Export of down-regulation capacity is provided by hydropower in SE1, SE2 and thermal power in SE4.

Fig. 7 shows the ratio between actual and minimum generation for all hydropower stations in the hydro-dominated bidding zone NO2 for week 31 in the dry and wet inflow year, sorted in decreasing order. Recall that the minimum generation was set to 50% of the best efficiency point, explaining the large percentage of time spent at a ratio of around 2.0. As expected the hydropower system is utilized to a much larger extent in the wet year. We observe that the differences in utilization between the cases with and without reserve exchange are less pronounced in the wet year. With the possibility to exchange reserves in the dry year, the reserve requirements in the short-term problem become less constraining, and some of the hydropower generation is reduced to save water for the future, as shown in Fig. 7.

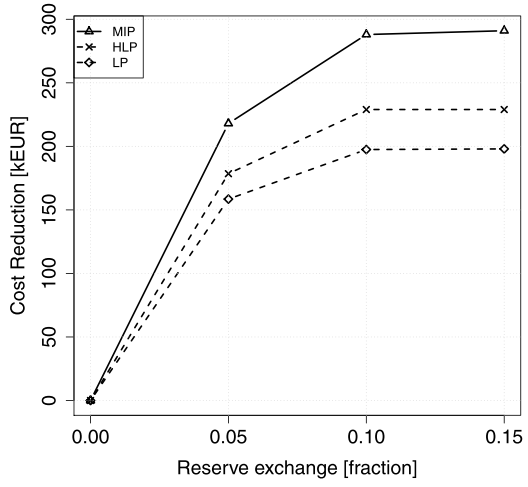

Fig. 4. Cost reduction (in k€) for different fractions of transmission capacity allowed for reserve exchange for a summer weekday in the wet inflow scenario.

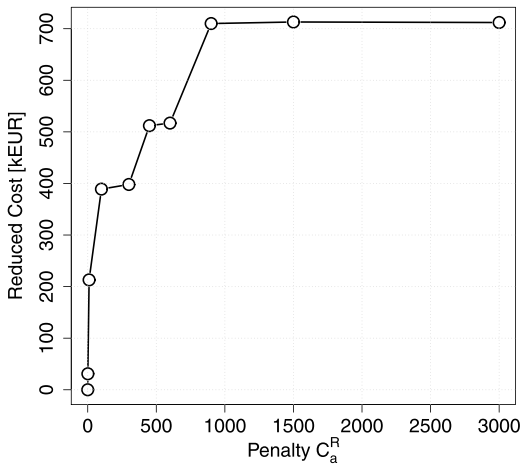

Fig. 5. Cost reduction due to reserve exchange (in k€) for different values of C_a^R for a weekday in week 31 in the dry inflow scenario.

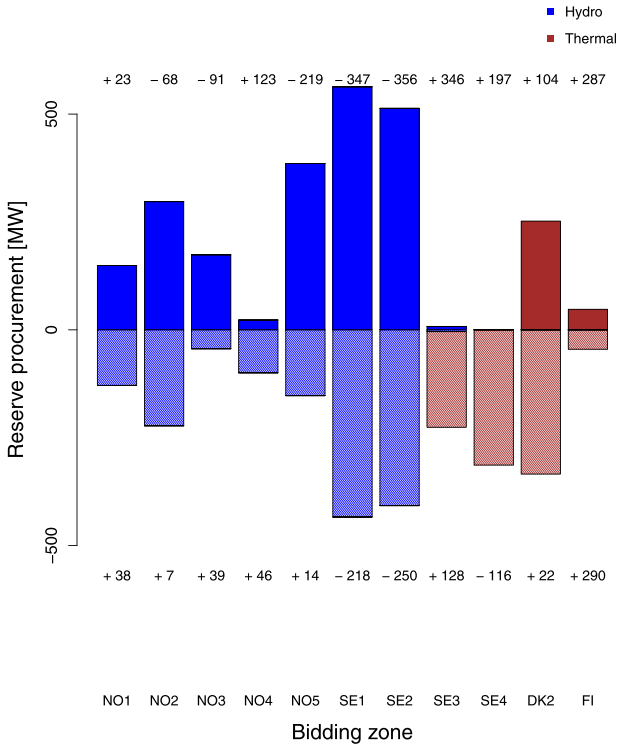

Fig. 6. Reserve procurement of up-regulating (positive) and down-regulating (negative) reserves per technology and per bidding zone for hour 9 for D1 in week 31 in the dry scenario. The net exchanges of reserves per bidding zone are indicated in the top (up-regulation) and bottom (down-regulation) of the figure, where a positive value means that the bidding zone imports reserve capacity, and vice versa.

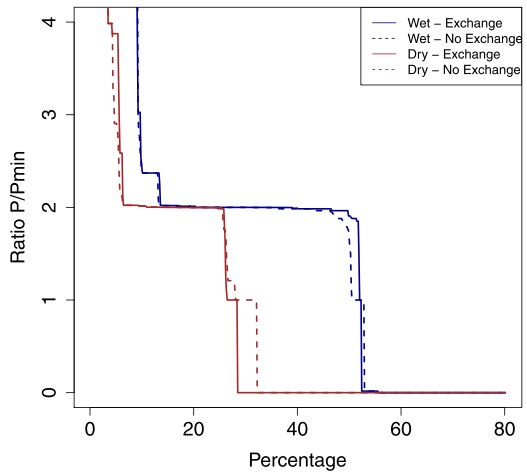

Fig. 7. Ratio between actual and minimum generation for all hydropower stations in bidding zone NO4 in week 31 in the dry (red) and wet (blue) inflow year, with 10% (solid-drawn) and no (stapled) reserve exchange between bidding zones. (For interpretation of the references to colour in this figure legend, the reader is referred to the web version of this article.)

4. Conclusions

We presented a hydrothermal scheduling toolchain combining long- and short-term models and applied it to quantify the benefit of exchanging spinning reserve capacity across bidding zones and countries in the Nordic power market. Considering a set of representative days in a data description of a 2030 scenario for the Northern European power system, we estimated that the average economic benefit by making 10% of the transmission grid capacity available for exchange of reserve capacity between bidding zones in the Nordic synchronous system to be 290 k€ /day. This number becomes significantly lower if reserves are to be shared within and exchanged between countries.

The case study demonstrates the importance of detailed modelling of both the hydro and thermal generation. In particular, the detailed representation of the hydropower is crucial for accurately capture the flexibility of the Nordic system to deliver spinning reserve capacity. By relaxing the integrality requirement for the unit commitment decision variables in the hydropower system, the economic benefit of reserve capacity exchange was on average reduced by 22%.

We emphasize that the case study results are subject to many assumptions regarding the market structure and system representation in the reference year 2030. The considered case comprises a substantial amount of new wind and solar power compared to today's system, and thus the estimated economic benefit of exchanging reserve capacity is not directly valid for today's system.

CRediT authorship contribution statement

Arild Helseth: Conceptualization, Methodology, Formal analysis, Visualization, Writing - original draft. **Mari Haugen:** Conceptualization, Methodology, Software, Data curation, Writing - review & editing. **Hossein Farahmand:** Conceptualization, Methodology, Writing - review & editing. **Birger Mo:** Conceptualization, Methodology, Writing - review & editing. **Stefan Jaehnert:** Conceptualization, Methodology, Writing - review & editing. **Inge Stenkløv:** Conceptualization, Writing - review & editing.

Declaration of Competing Interest

The authors declare that they have no known competing financial interests or personal relationships that could have appeared to influence the work reported in this paper.

Acknowledgment

This work was funded by The Research Council of Norway Project No. 268014.

References

[1] K. Van den Bergh, R.B. Hytowitz, K. Bruninx, E. Delarue, W. Dhaeseleer, B. F. Hobbs, Benefits of coordinating sizing, allocation and activation of reserves among market zones, Electr. Power Syst. Res. 143 (2017) 140–148.
[2] H. Farahmand, G. Doorman, Balancing market integration in the northern european continent, Appl. Energy 96 (2012) 316–326.
[3] Commission regulation (EU) 2017/2195 of 23 november 2017 establishing a guideline on electricity balancing, 2019, http://data.europa.eu/eli/reg/2017/2195/oj.
[4] N. Flatabø, G. Doorman, O.S. Grande, H. Randen, I. Wangensteen, Experience with the Nord Pool design and implementation, IEEE Trans. Power Syst. 18 (2) (2003) 541–547.
[5] R. Scharff, J. Egerer, L. Söder, A description of the operative decision-making process of a power generating company on the nordic electricity market, Energy Syst. 5 (2014) 349–369.
[6] A. Helseth, M. Fodstad, A.L. Henden, Balancing Markets and their Impacton Hydropower Scheduling. techreport TR A7558, SINTEF Energy Research, 2016.
[7] Statnett, Market and operations, http://www.statnett.no/en/Market-and-operations/.
[8] ENTSO-E, Explanatory document to the all TSOs' of CCR nordic proposal for a methodology for a market-based allocation process of cross-zonal capacity for the exchange of balancing capacity in accordance with (1) of commission regulation (EU) 2017/2195 of 23 november 2017 establishing a guideline on electricity balancing, 2019, https://www.entsoe.eu/.
[9] R.F. Carramolino, F. Careri, K. Kavvadias, I. Hidalgo-Gonzalez, A. Zucker, E. Peteves, Systematic mapping of power system models - Expert survey. Tech. rep. eur 28875 en, European Comission - Joint Research Centre, 2017.
[10] P. Meibom, H.V. Larsen, R. Barth, H. Brand, C. Weber, O. Voll, WILMAR deliverable d6.2 (b) WILMAR joint market model documentation. Tech. rep. risø-r-1552(en), Forskningscenter Risoe, 2006.
[11] H. Ravn, WILMAR deliverable d6.2 (c): The WILMAR long term model. Tech. rep., Risoe National Laboratory, 2006.
[12] P. Meibom, R. Barth, B. Hasche, H. Brand, C. Weber, M. O'Malley, Stochastic optimization model to study the operational impacts of high wind penetrations in ireland, IEEE Trans. Power Syst. 6 (3) (2011) 1367–1379.
[13] A. Bossavy, M. Chammas, J. Fauquet, M. Fender, L. Fournié, P. Khallouf, B. Texier, METIS Technical Note T6 - METIS Power System Module. Tech. rep., European Comission, 2017.
[14] K. Sakellaris, J. Canton, E. Zafeiratou, L. Fournié, METIS: An energy modelling tool to support transparent policy making, Energy Strategy Reviews 22 (2018) 127–135.
[15] T. Houghton, K.R.W. Bell, M. Doquet, Offshore transmission for wind: comparing the economic benefits of different offshore network configurations, Renew. Energy 94 (2016) 268–279.
[16] S. Mathieu, M. Petitet, M. Perrot, D. Ernst, Y. Phulpin, SiSTEM, a Model for the Simulation ofShort-Term Electricity Markets. Tech. rep. 30, Chaire European Electricity Markets, Paris-Dauphine University, France, 2017.
[17] A. Abbasy, R.A.C. van der Veen, R.A. Hakvoort, Effect of Integrating Regulating Power Markets of Northern Europe on Total Balancing Costs. Proc of IEEE PowerTech, Bucharest, Romania, 2009.
[18] S. Jaehnert, G. Doorman, Assessing the benefits of regulating power market integration in northern europe, International Journal of Electrical Power & Energy Systems 43 (1) (2012) 70–79.
[19] Y. Gebrekiros, G.L. Doorman, S. Jaehnert, H. Farahmand, Reserve procurement and transmission capacity reservation in the northern european power market, International Journal of Electrical Power and Energy Systems 67 (2015) 546–559.
[20] R. Domínguez, G. Oggioni, Y. Smeers, Reserve procurement and flexibility services in power systems with high renewable capacity: effects of integration on different market designs, International Journal of Electrical Power and Energy Systems 113 (2019) 1014–1034.
[21] S. Zalzar, E. Bompard, A. Purvins, M. Masera, The impacts of an integrated european adjustment market for electricity under high share of renewables, Energy Policy 136 (2020).
[22] Y. Gu, J. Bakke, Z. Zhou, D. Osborn, T. Guo, R. Bo, A novel market simulation methodology on hydro storage, IEEE Trans. Smart Grid 5 (2) (2014) 1119–1128.
[23] A. Helseth, B. Mo, A.L. Henden, G. Warland, Detailed long-term hydro-thermal scheduling for expansion planning in the nordic power system, IET Gener. Transm. Distrib. 12 (2) (2018) 441–447.
[24] M. Haugen, A. Helseth, S. Jaehnert, B. Mo, H. Farahmand, C. Naversen, On the Importance of Detailed Thermal Modeling for Price Forecasting in Hydro-thermal Power Systems. In Proc. of IEEE Canada Electrical Power and Energy Conference, 2019.
[25] J.W. Labadie, Optimal operation of multireservoir systems: state-of-the-art review, J. Water Resour. Plann. Manage. 130 (2) (2004) 93–111.
[26] A. Helseth, M. Haugen, S. Jaehnert, B. Mo, H. Farahmand, C. Naversen, Multi-market Price Forecasting in Hydro-thermal Power Systems. Proc. of 15th International Conference on the European Energy Market, Lodz, Poland, 2018.

[27] W.E. Hart, C.D. Laird, J.-P. Watson, D.L. Woodruff, G.A. Hackebeil, B.L. Nicholson, J.D. Siirola, Pyomo–optimization modeling in python 2nd, 67, Springer Science & Business Media, 2017.
[28] IBM ILOG CPLEX optimizer, http://www-01.ibm.com/software/.
[29] J. Kong, H.I. Skjelbred, O.B. Fosso, An overview on formulations and optimization methods for the unit-based short-term hydro scheduling problem, Electr. Power Syst. Res. 178 (2020).
[30] J.M. Morales, A.J. Conejo, H. Madsen, P. Pinson, M. Sugno, Integrating Renewables in Electricity Markets. International Series in Operations Research & Management Science volume 205, Springer, 2014.
[31] L.E. Schäeffer, B. Mo, I. Graabak, Electricity Prices and Value of Flexible Generation in Northern Europe in 2030. 13th International Conference on the European Energy Market, Ljubljana, Slovenia, 2019.
[32] I. Graabak, H. Svendsen, M. Korpås, Developing a Wind and Solar Power Data Model for Europe with High Spatial-temporal Resolution. Proc. of 51th International Universities Power Engineering Conference (UPEC), 2016.
[33] Plan to increase automatic frequency restoration reserve (aFRR), https://www.statnett.no/for-aktorer-i-kraftbransjen/systemansvaret/kraftmarkedet/reservemarkeder/sekundarreserver/.